Electrochemical Oxidation of Nickel–Phosphine Complexes of the Type $[Ni^{II}(\eta^5\text{-}C_5Ph_5)\{Ph_2PCH{=}C(O)R\}]$ (R = Ph, $(\eta^5\text{-}C_5H_4)Fe(\eta^5\text{-}C_5H_5)$). Direct and Indirect Generation of Nickel(III) and Nickel(II)–Cation Radical Species

A. Louati,*,† and M. Huhn‡

Laboratoire d'Electrochimie et de Chimie Physique du Corps Solide, URA au CNRS No. 405, Université Louis Pasteur, 4 rue Blaise Pascal, F-67070 Strasbourg Cédex, France, and Laboratoire de Chimie Minérale, URA au CNRS No. 405, Ecole Européenne des Hautes Etudes des Industries Chimiques de Strasbourg, 1 rue Blaise Pascal, F-67008 Strasbourg Cédex, France

Received November 18, 1992

The electrochemical oxidation of $[Ni^{II}(\eta^5\text{-}C_5Ph_5)\{Ph_2PCH{=}C(O)Ph\}]$ (**1**) and $[Ni^{II}(\eta^5\text{-}C_5Ph_5)\{Ph_2PCH{=}C(O)Fc\}]$ (Fc = Ferrocenyl group) (**2**) has been investigated in dichloromethane by rotating disk voltammetry, cyclic voltammetry, thin-layer spectroelectrochemistry, and ESR spectroscopy. At a platinum electrode, **1** undergoes a reversible one-electron oxidation whereas the oxidation of **2** proceeds by two successive reversible one-electron steps. The oxidation of **1** generates a $[Ni^{III}]^+$ species which is stable over 6 h in solution. For complex **2**, the first electron loss, based on a transient species proposed to involve the ferrocenyl center, triggers an intramolecular redox reaction, resulting in the formation of a $[Ni^{III}]^+$ species having a lifetime of ca. 1 h. In both cases, the formation of the $[Ni^{III}]^+$ complex is followed by an irreversible chemical reaction. All data suggest that this latter transformation involves an irreversible intramolecular electron transfer between the Ni^{III} center and the electron-rich enolate to give ultimately a Ni^{II}–cation radical complex.

Introduction

Ligands which contain a redox-active pendant site offer the possibility of tuning the reactivity of a metal center without altering the coordination sphere. This may be achived via controlled changes in the oxidation state of the redox center. Ferrocene-derived phosphine ligands have been shown to be suitable for the synthesis of bimetallic (Fe, M) systems allowing electronic communication.[1] Thus, we recently found that the electrochemical oxidation of the ferrocene moiety of the palladium complex **A** (Chart I) is followed by an internal electron transfer from the palladium(II) center to the ferrocenium group leading to an unstable $[Pd^{III}\text{–}Fe^{II}]^+$ species.[2] Aiming at the stabilization of ferrocenium-induced organotransition radicals, we envisaged the study of the binuclear complex **2** containing a C_5Ph_5 ligand. Perphenylated ligands have been shown to stabilize metals in unusual oxidation states,[3–5] and in the present case it can be anticipated that the $\eta^5\text{-}C_5Ph_5$ ligand may sterically stabilize a Ni^{III} species formed after a possible internal redox process. In order to determine the influence of the ferrocenyl center on the stability of an oxidized nickel center, we also investigated the electrochemical behavior of the parent mononuclear complex **1**.

Experimental Section

Voltammetric data were obtained with a standard three-electrode system, using either a potentiostat/galvanostat (EG&G PAR Model 273) interfaced with an AT Model 386 SX microcomputer or with a Bruker E 130 M potentiostat and a high-impedance millivoltmeter (minisis 6000, Tacussel). Current/potential curves were obtained either on a Hewlett-Packard or an Ifelec If 3802 X-Y recorder. The working electrode was a platinum disk (EDI type, Solea, Tacussel) of 3.14 mm^2 surface area. A platinum wire was used as the auxiliary electrode. In all cases, a saturated calomel electrode (SCE), connected to the solution by a bridge filled with CH_2Cl_2 + 0.1 M Bu_4NPF_6, was used as the reference; under the experimental conditions used $E°$ for the oxidation of ferrocene is 0.50 V. In the controlled-potential electrolyses, the anode and cathode compartments of the working cell were separated by a fritted glass disk. The working electrode was a platinum spiral wire (ϕ = 0.8 mm) 30 cm in length. The working potential was controlled by a PRT 100 potentiostat (Tacussel). Spectroelectrochemistry was performed with a Hewlett-Packard 8452A diode array spectrometer. The thin-layer spectroelectrochemical cell has been previously described.[6] The ESR spectra were recorded at X-band frequencies on a Bruker ER 420 spectrometer equiped with a variable-temperature accessory. The cation radicals were generated for ESR studies with ambient-temperature controlled-potential coulometry in CH_2Cl_2, and the solutions were transferred to ESR sample tubes under nitrogen. These samples were rapidly solidified at liquid-nitrogen temperature for analysis of their frozen-solution spectra.

Complexes **1** and **2** were prepared according to the methods reported earlier.[7] Spectroscopic grade dichloromethane (CH_2Cl_2, Merck) was used as received (transferred under Argon). Tetrabutylammonium hexafluorophosphate (Bu_4NPF_6, Fluka) was used as supporting electrolyte throughout this study. It was twice recrystallized from absolute ethanol and stored under vacuum at 70 °C. All experiments were carried out under an argon atmosphere.

Results and Discussion

Voltammetric Studies. In voltammetry at RDE, a single anodic wave is observed for **1** and a double wave for **2**. Both complexes present a cathodic wave. The characteristics of the voltammograms are summarized in Table I. For each wave, the limit current I_{lim} is proportional to $\omega^{1/2}$ (ω = angular velocity) and the concentration of the substrate; it shows that I_{lim} is diffusion controlled. Logarithmic analysis of each oxidation wave gave slopes indicating a reversible one-electron process. The cathodic wave is quasi-reversible; the E vs log $[III_d - I]$ plots are slightly

† Université Louis Pasteur.
‡ Ecole Européenne des Hautes Etudes des Industries Chimiques de Strasbourg.

(1) (a) Roman, E.; Castro, V.; Camus, M. *J. Organomet. Chem.* **1985**, *293*, 93. (b) Harvey, P. D.; Gan, L. *Inorg. Chem.* **1991**, *30*, 3229. (c) Miller, T. M.; Ahmed, K. J.; Wrighton, M. S. *Inorg. Chem.* **1989**, *28*, 2347.
(2) Louati, A.; Gross, M.; Douce, L.; Matt, D. *J. Organomet. Chem.* **1992**, *438*, 167.
(3) Lane, G. A.; Geiger, W. E.; Connelly, N. G. *J. Am. Chem. Soc.* **1987**, *109*, 402.
(4) Connelly, N. G.; Raven, S. J. *J. Chem. Soc., Dalton Trans.* **1986**, 1613.
(5) Connelly, N. G.; Geiger, W. E.; Lane, G. A.; Raven, S. J.; Rieger, P. H. *J. Am. Chem. Soc.* **1986**, *108*, 6219.
(6) Lin, X. Q.; Kadish, K. M. *Anal. Chem.* **1985**, *57*, 1498.
(7) Matt, D.; Huhn, M.; Fischer, J.; De Cian, A.; Kläui, W.; Tkatchenko, I.; Bonnet, M. *J. Chem. Soc., Dalton Trans.* **1993**, 1173.

0020-1669/93/1332-3601$04.00/0

Chart I

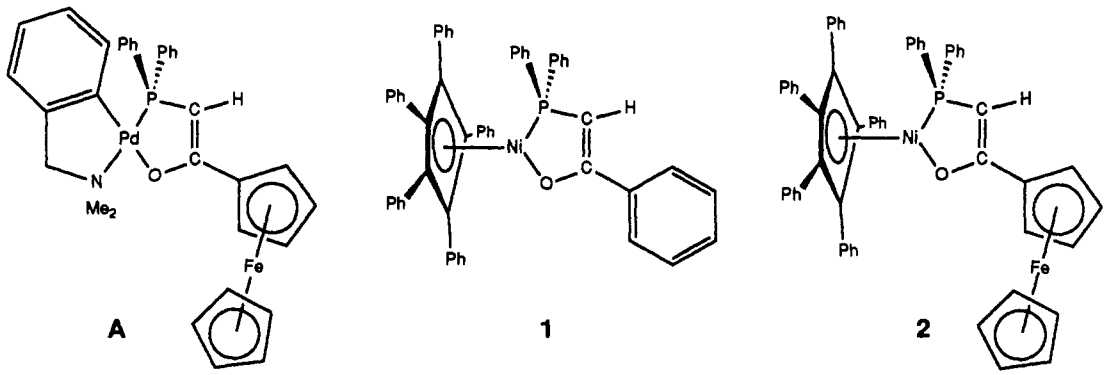

Table I. Electrochemical Parameters of **1** and **2** in Dichlormethane[a]

	oxidn step		redn step	
complex	$E_{1/2}$[b]	slope,[c] mV/log	$E_{1/2}$[b]	slope,[c] mV/log
1	0.52	65	−1.30	130
2	0.46	63	−1.29	120
	0.68	64		
A	0.47	66		
	1.32	88		
L[d]	0.73	88		

[a] Containing 0.1 M Bu_4NPF_6, complex concentration ca. 4.2×10^{-4} M, rotation rate = 1000 rev/min. [b] Volts vs SCE at 5 mV/s (platinum electrode); under the experimental conditions used $E°$ for the oxidation of ferrocene is 0.50 V. [c] Slope of E vs $\log(i/i_d - i)$ plot. [d] Uncomplexed ferrocenyl ligand: $[Ph_2PCH_2C(O)(\eta^5\text{-}C_5H_4)Fe(\eta^5\text{-}C_5H_5)]$.

curved with an average slope of ca. 120 mV. The number of electrons involved in each reduction and each oxidation were measured coulometrically and found to be one in both cases.

The literature data available for $[Ni^{II}Cp(phosphine)]$ complexes are scarce.[8] It is noteworthy that the $E_{1/2}$ values of the oxidation wave of **1** (0.52 V) and the second one of **2** (0.68 V) are close to those reported for other Ni^{II} complexes.[9,10] For both complexes, the $E_{1/2}$ values of the cathodic wave fall in the range observed for the reduction wave of most known nickel(II) complexes.[11-13]

The potential by itself measured for the first oxidation wave (0.46 V) of **2** does not allow an assignment of this wave. However, the spectroscopic observations made during the first and the second oxidation steps (UV–visible, ESR; *vide infra*), the comparison of the $E_{1/2}$ value with that of the $E_{1/2}$ value corresponding to the first oxidation step of complex **A** (Table I), and the analogy with numerous other ferrocenyl compounds,[1b,c,14,15] strongly suggest that the first oxidation wave of **2** is due to a transient species involving the ferrocenyl group. However, we emphasize that we have no direct proof for the formation of a ferrocenium ion (see below, spectroscopic characterization). For comparison, we also investigated the anodic behavior of the uncomplexed ferrocenyl ligand $[Ph_2PCH_2C(O)(\eta^5\text{-}C_5H_4)Fe(\eta^5\text{-}C_5H_5)]$ (**L**) using cyclic voltammetry. Over the entire scan rate range 0.5–5 V/s, **L** exhibited a single, ferrocenyl-based, reversible one-electron

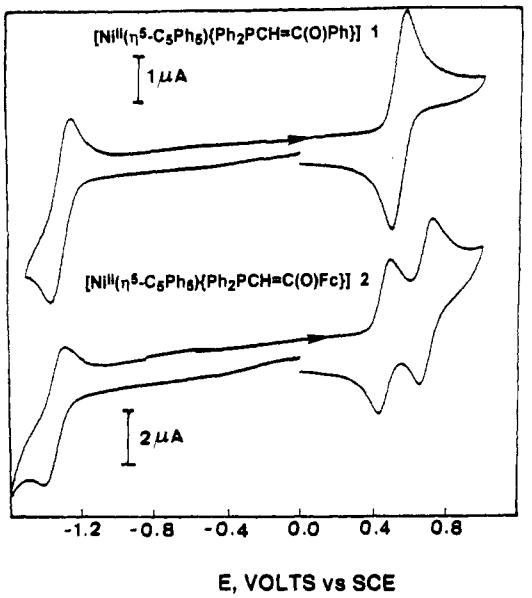

Figure 1. Cyclic voltammograms of **1** and **2** in CH_2Cl_2, 0.1 M Bu_4NPF_6 (scan rate 0.1 V/s).

oxidation (Table I). Interestingly, the first oxidation wave of **2** appears ~0.3 V more cathodic than the free ligand **L**. This is consistent with the presence in **2** of a negative charge (conjugate enolate) next to the ferrocenyl group. From Table I it can be seen that the second oxidation potential which may be ascribed to the nickel center is *ca.* 160 mV more anodic than that the oxidation potential of **1**. The shift to a more anodic potential results from the strong electron-attractive effect of the monocation generated in the first step.

The cyclic voltammograms of **1** and **2** in CH_2Cl_2 (0.1 M Bu_4NPF_6) are illustrated in Figure 1. As seen in this figure, for **1**, one reversible oxidation process occurs at $E_{pa} = 0.57$ V whereas, for **2**, two reversible oxidation processes occur, at $E_{pa} = 0.49$ and 0.72 V. For both complexes, one reduction step having a poor reversibility occurs at *ca.* −1.30 V.

In this study, only the first oxidation processes will be analyzed.

In Figure 2 are presented typical cyclic voltammograms of **1** in the range 0–1.2 V at different scan rates. At the lowest scan rates ($v \leq 1$ V/s; see Figure 2a), a well-defined reversible one-electron oxidation was observed (process 1) and a reversible process with reduced intensity at a more positive potential (process 2). At scan rates higher than 1 V/s, process 2 disappeared (see Figure 2c). For the main process 1, within the scan rate range 0.05–5 V/s, the peak current ratio of I_{pc}/I_{pa} remained close to 0.9, the difference $E_{pa} - E_{pa/2}$ increased from 60 to 90 mV, and the potential peak E_{pa} shifted positively by approximately 35 mV/10-fold increase in scan rate. The theoretical shift of E_p is 30 mV/log (scan rate) for a chemical reaction following electron transfer. These data are consistent with an EC type mechanism in which

(8) Koelle, U.; Werner, H. *J. Organomet. Chem.* **1981**, *221*, 367.
(9) Frisch, D. P.; Lloyd, M. K.; McCleverty, J. A.; Seddon, D. *J. Chem. Soc., Dalton Trans.* **1973**, 2268.
(10) Lovecchio, F. V.; Gore, E. S.; Busch, D. H. *J. Am. Chem. Soc.* **1974**, *96*, 3109.
(11) Edwin, J.; Bochmann, M.; Bôhm, M. C.; Brennan, D. E.; Geiger, W. E., Krûger, C.; Pebler, J.; Pritzkow, H.; Siebert, W.; Swiridoff, W.; Wadepohl, H.; Weiss, J.; Zenneck, U. *J. Am. Chem. Soc.* **1983**, *105*, 2582.
(12) Zwecker, J.; Kuhlmann, T.; Pritzkow, H.; Siebert, W.; Zenneck, U. *Organometallics* **1988**, *7*, 2316.
(13) Bowmaker, G. A.; Boyd, P. D. W.; Campbell, G. K. *Inorg. Chem.* **1982**, *21*, 2403.
(14) Kotz, J.; Neyhart, G.; Vining, W. J. *Organometallics* **1983**, *2*, 79.
(15) Colbran, S. B.; Robinson, B. H.; Simpson, J. *Organometallics* **1983**, *2*, 943.

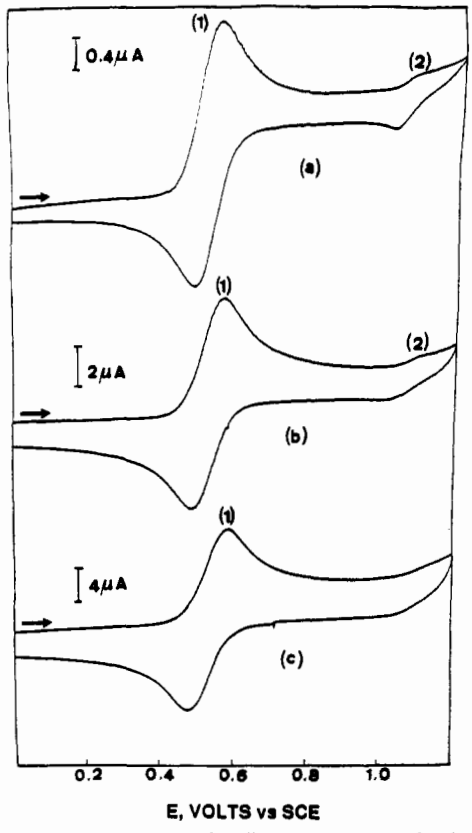

Figure 2. Scan rate dependence of cyclic voltammograms for the oxidation of 4.2×10^{-4} M **1** in CH_2Cl_2, 0.1 M Bu_4NPF_6. Scan rates: (a) 0.05 V/s; (b) 0.5 V/s; (c) 2 V/s.

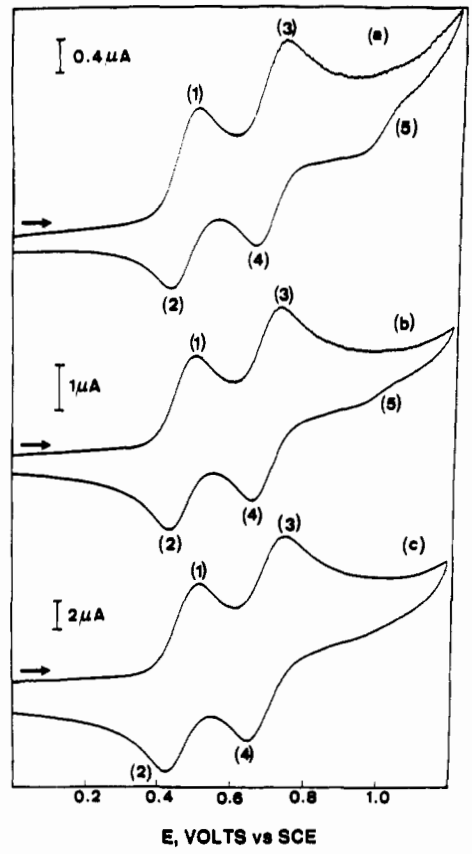

Figure 3. Scan rate dependence of cyclic voltammograms for the first oxidation of 4.2×10^{-4} M **2** in CH_2Cl_2, 0.1 M Bu_4NPF_6. Scan rates: (a) 0.05 V/s; (b) 0.1 V/s; (c) 1 V/s.

the electrochemical reaction (the E step) involves a reversible abstraction of one electron.[16]

Representative cyclic voltammograms of **2** are shown in Figure 3. On the anodic portion of the voltage scan ($v \leq 0.1$ V/s, Figure 3a), peaks 1 and 3 are found having peak potentials of 0.49 and 0.73 V. The cathodic portion of the voltage scan displays a reduction wave 5 at about 1.0 V and two reduction peaks 2 and 4 at 0.43 and 0.65 V, which correspond to the reduction of the products formed at the first and the second oxidation steps, respectively. From $v = 0.1$ V/s (Figure 3b), the current for process 5 begins to disappear and vanishes completely at scan rates higher than 1 V/s (Figure 3c) while, at the same time, the intensity of peak 4 increases. The competitiveness of peaks 4 and 5 suggests that the former peak should be associated with the chemically reversible reduction of the species generated in the anodic charge transfer. Note also that the $I_p(2)/I_p(1)$ ratio decreased (0.9–0.55) while $I_p(4)/I_p(3)$ increased (0.95–1.4) with increasing scan rate. A study of the first oxidation step between 0 and 0.6 V over a wide range of moderate scan rates (0.05–1 V/s), shows that this step has all the properties of a quasi-reversible one-electron transfer;[16] thus, (i) $\Delta E_p = E_{pa} - E_{pc} = 80 \pm 5$ mV, (ii) $E_p^{ox} - E_{p/2}^{ox} = 60 \pm 5$ mV, and (iii) the anodic and cathodic peaks currents are approximately equal in height. From these data it can be concluded that the initial charge transfer to form the one-electron oxidized product is rapid (diagnostic: $E_p^{ox} - E_{p/2}^{ox}$) and that the cation radical undergoes an irreversible chemical reaction.

Spectroelectrochemical Characterization of Oxidation Sites. Electronic absorption spectra were monitored during the controlled-potential electrolysis of each complex, and typical time-resolved thin-layer spectra are shown in Figure 4.

Spectra obtained during oxidation of **1** at 0.75 V are shown in Figure 4a. As the oxidation of **1** proceeds, the absorption bands at 318 and 380 nm decreased while a new broad band, centered at *ca.* 464 nm with several shoulders, appeared. This band which resembles the d–d transitions of other Ni^{III} complexes[17,18] suggests that the charge transfer occurs at the metal center (i.e. Ni^{II}). The presence of one isosbestic point at 414 nm indicates that only the oxidized $\mathbf{1}^+$ is generated in solution.

The oxidation of complex **2** was followed using the same procedure. The fixed potential was 0.42 V, corresponding to a value slightly below the first oxidation step. The observed spectral changes are shown in Figure 4b for this oxidation in CH_2Cl_2. Three distinct isosbestic points are present at 336, 360, and 398 nm, thus indicating the formation of only one new species during the first oxidation step of **2**. The spectral changes shown in Figure 4c were obtained during the two oxidations of **2** (the potential was scanned from 0 to 0.9 V). The absorption bands at 314 and *ca.* 370 nm decreased, and a new absorption peak between 450 and 500 nm increased to give a broad peak centered at about 472 nm (compare with Figure 4a). The original spectrum of **2** could be reversibly regenerated during the return potential sweep. The comparison of the spectrum of Figure 4a with that of Figure 4c strongly suggests that the second oxidation step may be attributed to the oxidation of the nickel center. As a consequence, the first step is likely to correspond to the oxidation of the ferrocenyl moiety, although a typical Fc^+ absorption band near 620 nm could not be detected. The absence of this band (see Figure 4b) occurs frequently with mixed-valence compounds containing the ferrocenium moiety.[15,19]

When both $\mathbf{1}^+$ and $\mathbf{2}^+$ were reduced, the original spectra of **1** and **2**, respectively, were obtained. This demonstrates the full

(16) Nicholson, R. S.; Shain, I. *Anal. Chem.* **1964**, *36*, 706.

(17) Bhattacharyya, S.; Bose, S.; Basu, S. *J. Inorg. Nucl. Chem.* **1970**, *32*, 1032.

(18) Pavlik, I.; Cerny, V.; Maxova, E. *Collect. Czech. Chem. Commun.* **1970**, *35*, 3045.

(19) (a) Cowan, D. O.; Le Vanda, C.; Park, J.; Kaufman, F. *Acc. Chem. Res.* **1973**, *6*, 1. (b) Brown, G. M.; Meyer, J. T.; Cowan, D. O.; Le Vanda, C.; Kaufman, F.; Roling, P. V.; Rausch, M. D. *Inorg. Chem.* **1975**, *14*, 506.

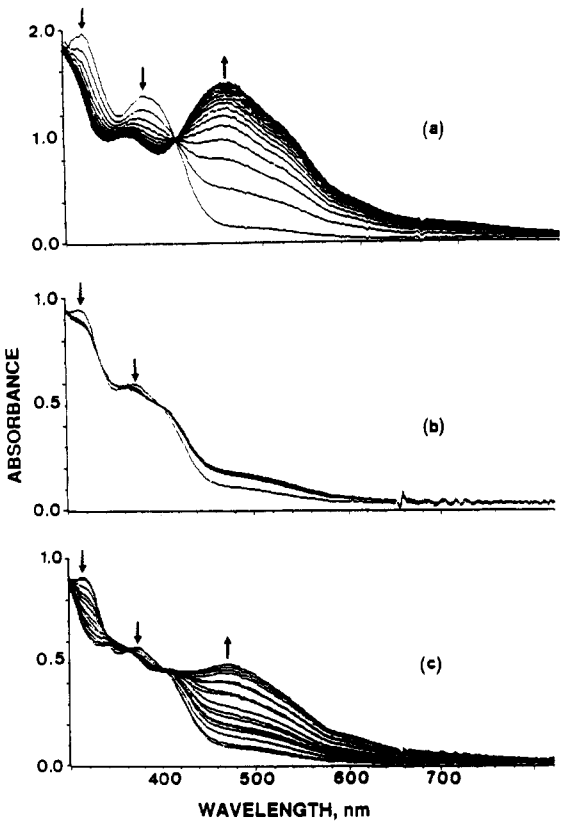

Figure 4. Thin-layer spectra in CH_2Cl_2 containing 0.1 M Bu_4NPF_6 during (a) controlled-potential oxidation of **1** at 0.75 V, (b) controlled-potential oxidation of **2** at 0.42 V, and (c) scanning of the potential from 0 to 0.9 V.

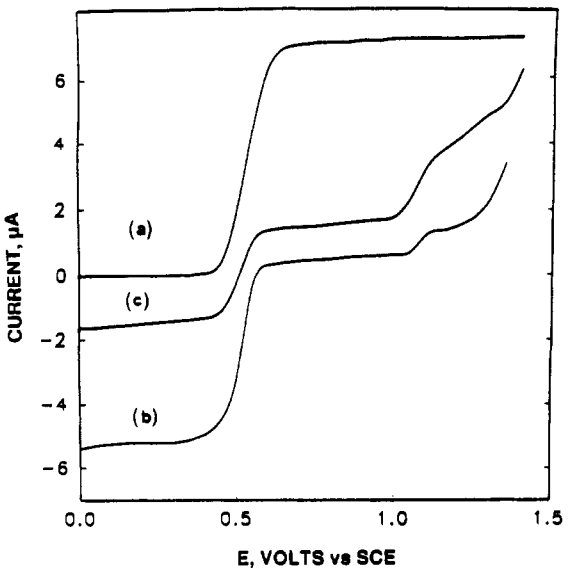

Figure 5. Voltammograms at a rotating disk electrode of **1** in CH_2Cl_2, 0.1 M Bu_4PF_6 (rotation rate 1000 rev/min): (a) Before electrolysis, (b) After controlled-potential oxidation at 0.65 V, and (c) 3–4 h after the end of the electrolysis.

stability of 1^+ and 2^+ as well as the reversibility of the processes on the thin-layer spectroelectrochemical time scale.

Characterization of Oxidation Products. On bulk electrolysis at 0.65 V, a yellow-orange solution of **1** in CH_2Cl_2 (0.1 M Bu_4NPF_6) became dark red-brown during the consumption of 0.95 F/mol. The cathodic scan of the solution obtained showed, as expected, a cathodic wave of which the half-wave potential is $E_{1/2} = 0.52$ V and a small anodic wave at *ca.* 1.05 V (Figure 5b). This result confirms the above reported reversibility of the oxidation step of **1** and suggests the generation of a rare Ni^{III}–phosphine complex.[20] The height of the cathodic wave is inferior to that which would have theoretically been expected. This is consistent with the chemical reaction detected by cyclic voltammetry. The red-brown 1^+ ion is considerably stable. Indeed, several hours after the coulometry at 0.65 V is completed (3–4 h), the cathodic wave is still well defined (Figure 5c) but the oxidation current for the process at *ca.* 1.05 V increased. Finally, 6–7 h after the end of the electrolysis, the cathodic wave had vanished. Only the anodic wave at *ca.* $E_{1/2} = 1.05$ V and some minor waves near 1.2 V were present. This indicates that the Ni^{III} species had mainly converted into a new complex having a poorly reversible oxidation process at $E_p = 1.10$ V ($v = 0.1$ V/s). Two cathodic processes at $E_p = -0.43$ and -1.45 V are associated with this new species. The process at $E_p = -0.43$ V is likely to correspond[21] to a ligand-centered reduction of this species. Bulk coulometry of the final solution at -0.6 V led to partial re-formation of the starting material.

The solution obtained after the exhaustive coulometric oxidation of **1** was examined by UV–visible spectroscopy in the 300–800-nm range. Worthy of note is a strong, broad absorption band centered at 468 nm and a very weak band at about 700 nm. These results fit well with literature data[22,23] on Ni^{III} systems and confirm that the oxidation in **1** involves the nickel center. As time went on, the absorption bands due to Ni^{III} complex diminished and two others ($\lambda_1 = 320$ nm, $\lambda_2 = 404$ nm) grew in. After *ca.* 5 h, the final spectrum contained mainly these new bands. This indicates that the Ni^{III} species had completely converted into another compound. The spectrum of the final species is similar in shape to that of **1** (two bands in the range 300–800 nm) and suggests the formation of a Ni^{II}–cation radical species; the observed red shift (*ca.* 25 nm) of one of the bands of 1^+ (at 404 nm) vs that of **1** (at 380 nm) is consistent with an additional positive charge localized over a π system. It is noteworthy that the final electronic spectrum of the observed transformation displays no bands either at 626 nm[24] or at 584 nm,[25] expected for the blue $[C_5Ph_5]^{+\bullet}$ cation radical and the purple free $[C_5Ph_5]^{\bullet}$ radical, respectively.

ESR spectra of the solution were taken after electrolysis of **1**. At 120 K, the ESR spectrum (Figure 6a) displays one central strong line flanked by two signals at the g values of 2.165 and 2.001. The comparison of the g values $g_1 = 2.001$, $g_2 = 2.059$, and $g_3 = 2.165$ with literature data[26–32] allows to conclude that the ESR spectrum shown in Figure 6a is clearly due to a Ni^{III} species. After *ca.* 4 h, the ESR signals due to the Ni^{III} complex were still well defined (Figure 6b), confirming that the Ni^{III} complex is considerably stable. However, 6–7 h after the end of the electrolysis, the ESR signals due to the Ni^{III} complex disappeared and a typical free-electron signal ($g = 2.003$ and a width of 6.7 G) appeared (Figure 6c). This result confirms that the Ni^{III} species had been converted into another paramagnetic compound. The final ESR spectrum was examined over the

(20) The number of reports about Ni^{III}–phosphine complexes is very limited; see for exemple: Gray, R. L.; Higgins, S. J.; Levason, W.; Webster, M. *J. Chem. Soc., Dalton Trans.* **1984**, 459.
(21) Lane, G.; Geiger, W. E. *Organometallics* **1982**, *1*, 401.
(22) Warren, L. F.; Bennett, M. A. *Inorg. Chem.* **1976**, *15*, 3126.
(23) Van Hecke, G. R.; Horrocks, D. W., Jr. *Inorg. Chem.* **1966**, *5*, 1968.
(24) This value was determined after electrolysis at 1.2 V/SCE of a solution of C_5Ph_5Br.
(25) (a) Kurreck, H.; Broser, W. *Chem. Ber.* **1965**, *98*, 11. (b) This radical was obtained by reaction of BuLi with C_5Ph_5Br in THF.
(26) Davison, A.; Edelstein, N.; Holm, R. H., Maki, A. H. *J. Am. Chem. Soc.* **1963**, *85*, 2029.
(27) Stiefel, E. I.; Wate, J. H.; Billig, E.; Gray, H. B. *J. Am. Chem. Soc.* **1965**, *87*, 3016.
(28) Drago, R. S.; Baucom, E. I. *Inorg. Chem.* **1972**, *11*, 2064.
(29) Bernstein, P. K.; Gray, H. B. *Inorg. Chem.* **1972**, *11*, 3035.
(30) Sethulakshmi, C. N.; Subramainan, S.; Bennett, M. A.; Manoharan, P. T. *Inorg. Chem.* **1979**, *18*, 2520.
(31) Balasivasubramanian, E.; Sethulekshmi, C. N.; Manoharon, P. T. *Inorg. Chem.* **1982**, *21*, 1684.
(32) Chavan, M. Y.; Meade, T. J.; Busch, D. H.; Kuwana, T. *Inorg. Chem.* **1986**, *25*, 314.

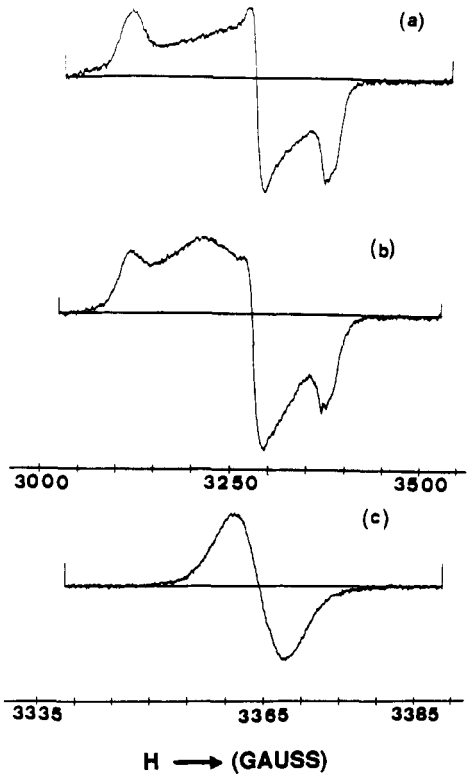

Figure 6. ESR spectra obtained at 120 K (a) immediately after controlled-potential oxidation of **1** in CH_2Cl_2, 0.1 M Bu_4NPF_6 at 0.65 V, (b) 4 h after the end of the electrolysis, and (c) 6–7 h after the end of the electrolysis.

temperature range 120–230 K. It is temperature independent and displays no secondary paramagnetic species. We note in particular the absence of the free cation radical $[C_5Ph_5]^{+\bullet}$ and that of the free radical $[C_5Ph_5]^{\bullet}$ (both usually characterized by the $\Delta m = 1$ transitions of the triplet state and the $\Delta m = 2$ (half-field) transition).[33-35] The g factor and linewidth imply that the final product should be formulated as a nickel(II)–ligand stabilized cation radical (Ni^{II}–$L^{+\bullet}$) species.

Finally, the one-electron exhaustive coulometric oxidation of **1** was repeated, and the solution was evaporated. The FAB-MS spectrum contains a dominant molecular ion (m/z 806.8, 100% intensity) consistent with the presence of $[Ni^{II}(\eta^5\text{-}C_5Ph_5)\text{-}\{Ph_2PCH{=}C(O)Ph\}]^+$ species (and not **1** + H^+).

In the case of complex **2**, coulometry was carried out at E = 0.47 V corresponding to the first oxidation wave.[36] The oxidation was accompanied by a color change from yellow-orange to dark red-brown; the number of electrons exchanged (n) was found to be 1. After electrolysis, the original oxidation wave at $E_{1/2}$ = 0.46 V (Figure 7a) had become a reduction wave, with rotating platinum electrode scans giving a plateau height of about 50% of the original wave (Figure 7b). This result confirms partially the above reported reversibility of the first oxidation step of **2** and the occurrence of some chemical side reactions. Several minutes after the coulometry was completed (10–15 mn), this wave (Figure 7b) had "shifted" to more positive potentials giving a new mixed oxidation–reduction wave (Figure 7c) with $E_{1/2}$ = 0.72 V. This value suggests a $[Ni^{II}] \rightarrow [Ni^{III}]$ transformation (compare with Figure 7a) produced by an internal electronic exchange. Finally, 1 h at most after the end of the electrolysis, the latter mixed wave had disappeared and only oxidation processes were observed by cyclic voltammetry (Figure 8). As shown in Figure 8, two

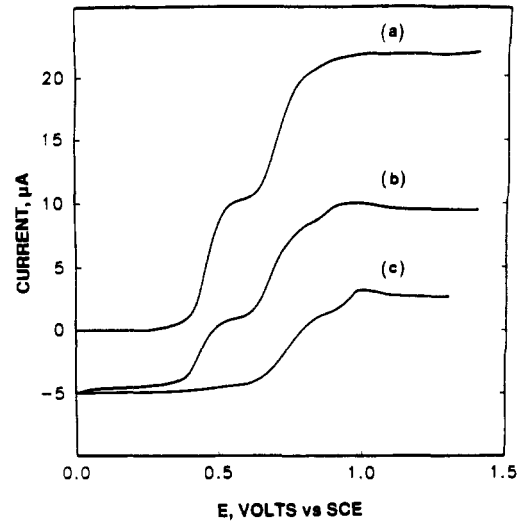

Figure 7. Rotating disk voltammograms of **2** in CH_2Cl_2, 0.1 M Bu_4NPF_6 (rotation rate 1000 rev/min): (a) Before electrolysis, (b) after consumption of one electron/molecule at 0.47 V, and (c) 10–15 min after the end of the electrolysis.

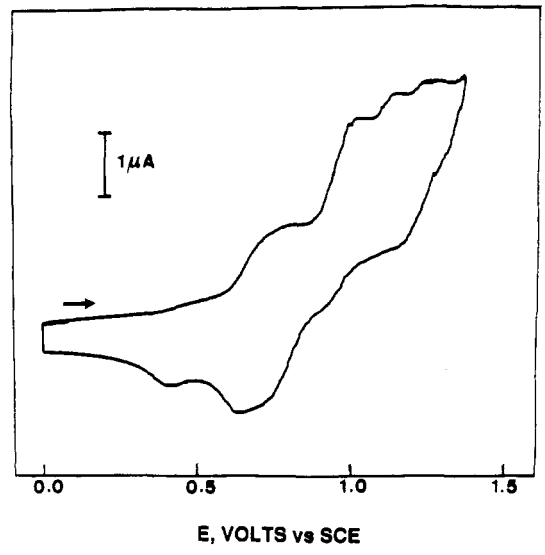

Figure 8. Cyclic voltammogram of the oxidized product of **2** obtained 1 h after the end of the electrolysis of **2** at 0.47 V.

reversible oxidation steps at E_p = 0.80 and 1.10 V were observed. It should be furthermore mentioned that the CV scan (not shown) showed three cathodic processes at E_p = –0.47, –0.65, and –1.45 V. The peak potentials at –0.43 and –1.45 V are consistent with those expected for a $[Ni^{II}\text{–}Fe^{II}]^+$ species. That at –0.65 V/SCE could not be identified. An exhaustive reduction of the final solution at –0.53 V led to partial regeneration of **2**.

The electronic spectrum in the 300–800-nm range of the solution obtained after oxidative electrolysis of **2** at 0.47 V displayed several bands, notably a band at 470 ± 5 nm which indicates the formation of a transient Ni^{III} species.[37] This band disappeared with time, indicating the conversion of the Ni^{III} species. The spectrum of the final product showed well-defined absorption bands at 322 and 410 nm, typical for a $[Ni^{II}\text{–}L^{+\bullet}]$ species. As for the UV–visible study performed for **1**, no bands due to the free cation radical $[C_5Ph_5]^{+\bullet}$ or free radical $[C_5Ph_5]^{\bullet}$ could be detected.

ESR measurements (T = 120 K) were performed on a solution of **2** *during* controlled-potential oxidation at 0.47 V in CH_2Cl_2 (0.1 M Bu_4NPF_6). The signal in Figure 9a was obtained 10 min after that oxidation potential was applied. It is centered at g =

(33) Breslow, R.; Chang, H. W.; Yager, W. A. *J. Am. Chem. Soc.* **1963**, *85*, 2033.
(34) Breslow, R.; Hill, R.; Wasserman, E. *J. Am. Chem. Soc.* **1964**, *86*, 5349.
(35) Broser, W.; Kurreck, H.; Siegle, P. *Chem. Ber.* **1967**, *100*, 788.
(36) The applied potential (0.47 V/SCE) was choosen so as to avoid the oxidation of the nickel center.

(37) In view of the fact that λ_{max} remained unchanged on using acetonitrile instead of CH_2Cl_2, this latter band may be assigned to a d–d transition.

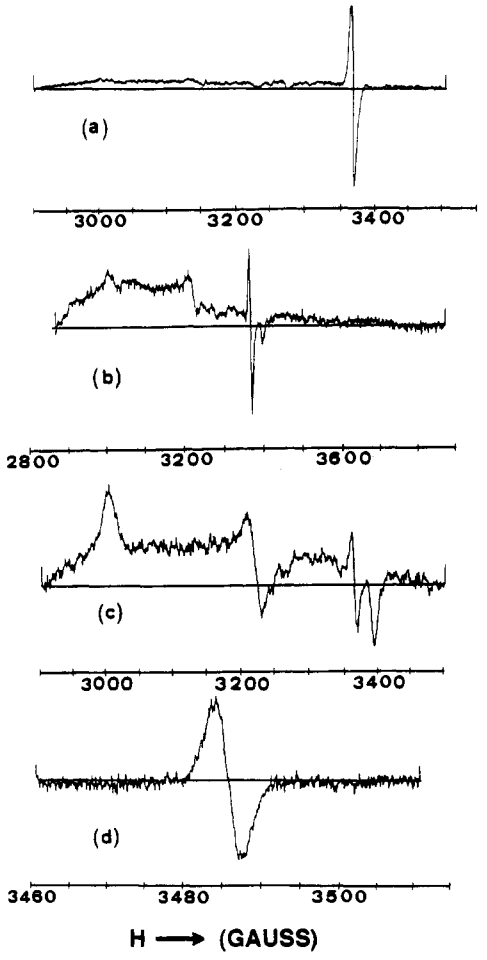

Figure 9. ESR spectra obtained at 120 K during oxidation of **2** in CH_2Cl_2, 0.1 M Bu_4NPF_6: (a) 10 min after the applied potential 0.47 V, (b) after one-electron exchange, (c) *ca.* 30 min after the end of the electrolysis, and (d) 1 h after the end of the electrolysis.

2.003 and has a width of 7 G. The intensity of this signal continues to increase when the applied potential is held constant at 0.47 V. The spectrum obtained once the abstraction of one electron/mol of **2** is achieved (as determined by integration of the current–time curve) is shown in Figure 9b. It still displays the strong signal with $g = 2.003$. This signal is distinct from that expected for a Fc^+ species. The ferrocenium compounds have been reported[38] to have $g_\parallel$ in the range 3.2–4.35 and $g_\perp$ in the range 1.91–1.26. Thus, the signal observed after one-electron oxidation of **2** resembles rather that of an organic radical. Interestingly, we established that the intensty of this signal is ~70% of the intensity expected if all 2^+ cation radical in the solution contributed to the signal. Due to the fact that enolato–phosphines in nickel and palladium complexes may behave as hemilabile ligands[39] and therefore favor an equilibrium of the type $2 \rightleftharpoons 2'$ (see $2 \rightleftharpoons 2'$ equilibrium in Scheme II), it is likely that once ferrocenium is formed, a fast electron exchange with the neighboring enolato function occurs. Such a transfer is highly favored by the close proximity of a negative charge located on the oxygen atom of **3** (see Scheme II). This hypothesis could explain the failure of the observation of typical ferrocenium signals but only that of an organic-type radical.

(38) (a) Duggan, D. M.; Hendrickson, D. N. *Inorg. Chem.* **1975**, *14*, 955. (b) Prins, R.; Reinders, F. J. *J. Am. Chem. Soc.* **1969**, *91*, 4929. (c) Prins, R. *Mol. Phys.* **1970**, *19*, 603. (d) Prins, R.; Korswagen, A. R. *J. Organomet. Chem.* **1970**, *25*, C74. (e) Prins, R.; Kortbeek, A. G. T. G. *J. Organomet. Chem.* **1971**, *33*, C33. (f) Cowan, D. O.; Candela, G. A.; Kaufman, F. *J. Am. Chem. Soc.* **1971**, *93*, 3889. (g) Horsfield, A.; Wassermann, A.; Ramsey, W.; Forster, R. *J. Chem. Soc. A* **1970**, 3202.

(39) Bader, A.; Lindner, E. *Coord. Chem. Rev.* **1991**, *108*, 27 and references therein.

Scheme I. Proposed Reaction Scheme for the Oxidation of **1**

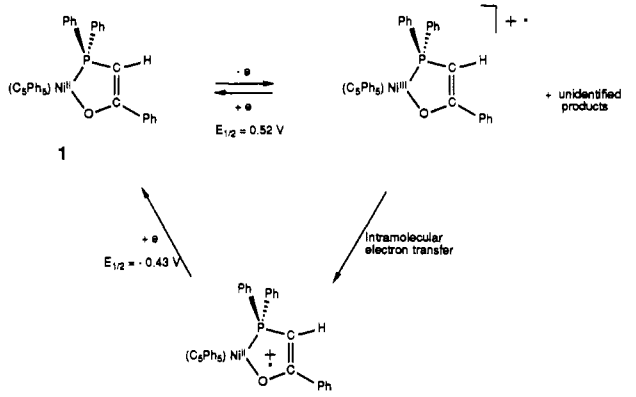

In addition, the spectrum (Figure 9b) shows three weak signals characterized by $g_1 = 2.24$, $g_2 = 2.091$, and $g_3 = 1.999$; this pattern is similar to that described above for a Ni^{III} species obtained by oxidation of **1** (Figure 6a). This indicates that there is a mixture of products, one of them corresponding to a Ni^{III} species. The signals of this latter species increase in intensity upon interruption of polarization while the strong signal (g = 2.003 and a width of 7 G) decreases (Figure 9c). Also after *ca.* 1 h, the signals of the Ni^{III} species had disappeared. Instead, a single signal (Figure 9d) was present ($g = 2.002$ and a width of 4.0 G) which is very similar to that observed for $\mathbf{1}^+$ several hours after the end of the electrolysis. This signal which is temperature independent between 120 and 230 K is characteristic of Ni^{II}–ligand-centered cation radical species. This is also consistent with the UV–visible data (see above), as well as the FAB-MS spectrum of a solution of **2** after one-electron exhaustive coulometry showing a peak at 914 (100% intensity), which corresponds to the cation $[Ni^{II}(\eta^5\text{-}C_5Ph_5)\{Ph_2PCH{=}C(O)Fc\}]^+$ species (and not $\mathbf{2} + H^+$). It should be noted that the chemical oxidation with Ag^+ of **2** led to the protonated parent complex $[Ni^{II}(\eta^5\text{-}C_5Ph_5)\{Ph_2PCH_2C(O)Fc\}]^+$ as the major product.[7]

Overall Oxidation Reaction Schemes for 1 and 2. Analysis of the electrochemical data coupled with the electronic absorption and the ESR spectra shows that the oxidation of **1** (Scheme I) is centered at the nickel atom. The thus formed Ni^{III} species which has a stability of *ca.* 6–7 h slowly undergoes a transformation into a Ni^{II}–ligand centered cation radical which in turn may be reduced to **1**.

In the case of complex **2** (Scheme II), the first oxidation process corresponds to the formation of a transient species proposed to involve the ferrocenyl center (**3**) (only observed on the CV time scale), which is rapidly converted to a transient radical ("enolate") species (**4**) (observed by ESR on the exhaustive coulometry time scale). This latter may itself act as an oxidant in an intramolecular oxidation (internal redox mediator) toward the Ni^{II} center, leading to a transient $[Ni^{III}\text{–}Fe^{II}]^+$ species **5**. Such intramolecular transfers have already been reported for other oxidized ferrocenyl compounds.[2,40–42] On the basis of the potentials for the one-electron oxidation of the Ni^{II} center ($E_{1/2}$ = 0.68 V) and the one-electron reduction of the oxidized ferrocenyl moiety ($E_{1/2}$ = 0.46 V), the internal redox reaction would seem unfavorable. However, the closeness (<0.3 V) of the potentials and the presence of the conjugated enolate function, which may play the role of an electron-conducting bridging group, allow internal oxidative reaction to occur.[43] The $[Ni^{III}]^+$ species **5** thus formed is rapidly

(40) Pilloni, G.; Longato, B.; Corain, B. *J. Organomet. Chem.* **1991**, *420*, 57.
(41) Degrand, C.; Radecki-Sudre, A.; Besançon, J. *J. Electroanal. Chem., Interfacial Electrochem.* **1984**, *160*, 199.
(42) Degrand, C.; Radecki-Sudre, A. *J. Organomet. Chem.* **1984**, *268*, 63.
(43) Such phenomena have been observed in other bimetallic systems in which the metal centers are linked by a conjugated bridging ligand; see for example: Colbran, S. B.; Robinson, B. H.; Simpson, J. *Organometallics* **1983**, *2*, 952.

Scheme II. Proposed Reaction Scheme for the Oxidation of **2**

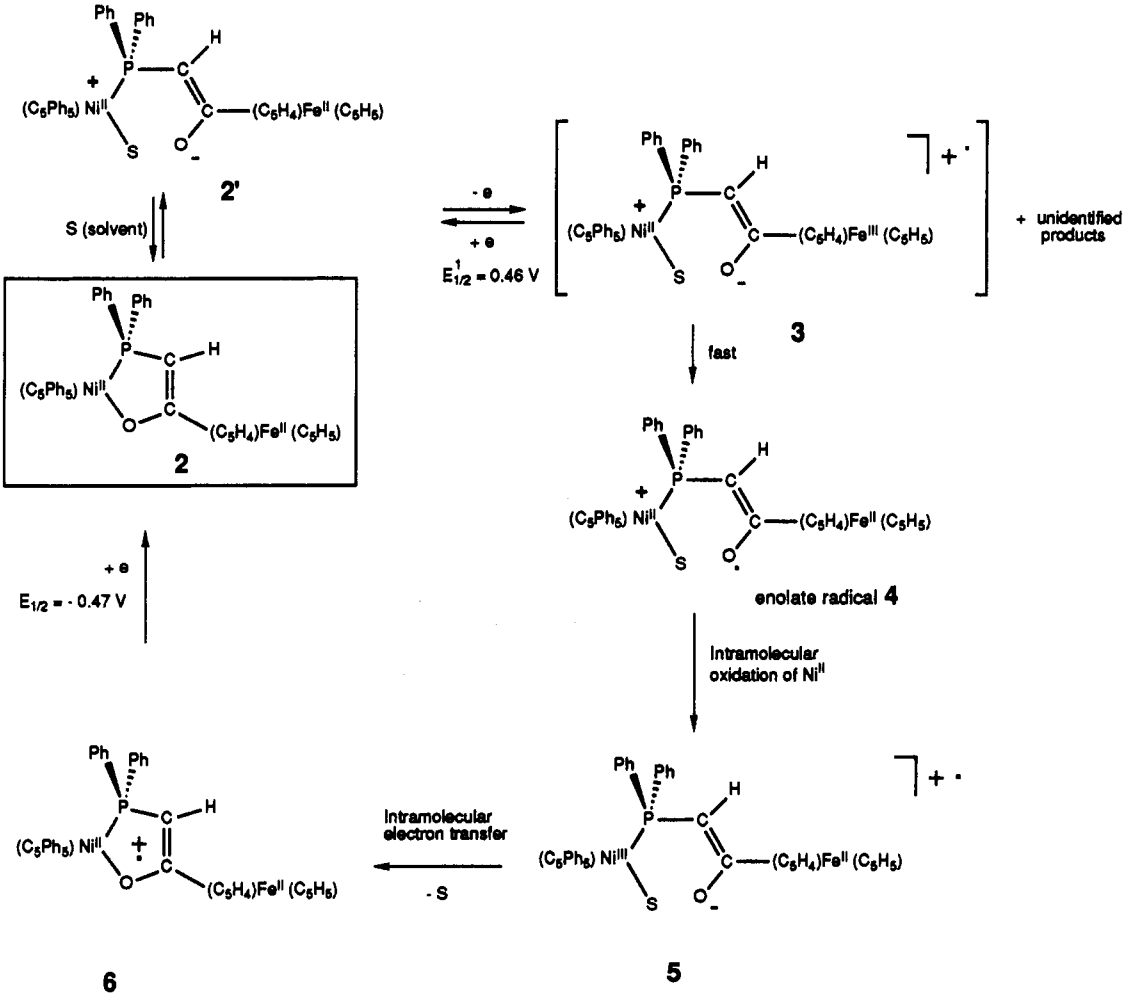

converted into a Ni^{II}–ligand-centered cation radical **6**, which may be reduced to **2**.

Thus, in this oxidation process, all that is detected is the radical ("enolate") and the interconversions of the complex to the nickel(III) complex followed by formation of the metal complex radical cation. The main evidence for these steps is a combination of ESR and electrochemistry.

Interestingly, the formation of the final $[Ni^{II}–L^{+\bullet}]$ species after electrolysis occurs faster in the case of **2** than that of **1**. This is consistent with the higher electron donor ability of the ferrocenyl center vs the phenyl group,[44,45] allowing an efficient stabilization of the final cation radical. The latter is likely to be localized within the nickelocycle since the ease of formation from the corresponding $[Ni^{III}]^+$ intermediate depends on the nature of the neighboring R group.

Acknowledgment. We are very grateful to Dr. D. Matt for helpful discussions.

(44) Connor, J. A.; Jones, E. M.; Lloyd, J. P. *J. Organomet. Chem.* **1970**, *24*, C20.
(45) Connor, J. A.; Lloyd, J. P. *J. Chem. Soc., Dalton Trans.* **1972**, 1470.